High-pressure metallic phases of boron

C. Mailhiot, J. B. Grant, and A. K. McMahan
Lawrence Livermore National Laboratory, Livermore, California 94550
(Received 13 June 1990)

First-principles total-energy calculations for solid boron predict a transition from the insulating α-rhombohedral phase first to a metallic body-centered-tetragonal structure at 210 GPa and subsequently to a face-centered-cubic structure at 360 GPa. While the possibility of intervening phases not considered here cannot be ruled out, it is argued that 210 GPa is an upper bound for the onset of a sequence of structural transitions by which boron evolves from a covalent insulator to a trivalent metal more like its neighbor Al.

I. INTRODUCTION

There is ample experimental[1–4] and theoretical[5–8] evidence that the application of pressure is inimical to the covalent bond. In a general argument, localization of charge in the covalent bond minimizes the potential energy at the expense of the kinetic energy. Given the respective $V^{-1/3}$ and $V^{-2/3}$ scaling of the potential and kinetic energy contributions with volume V, the latter must eventually dominate as V decreases, favoring more uniform electron density and more close-packed structures. The covalent, diamond-phase, group-IV semiconductors Si and Ge, for example, transform to metallic β-tin phases, and then after several further intermediate steps, culminate under 40 and 102 GPa, respectively, in close-packed metallic forms.[1,2] The covalent, threefold-coordinated, group-V solids P and As undergo analogous transitions reaching sixfold coordination under the largest pressures to which they have so far been investigated.[3,4]

We are concerned in this paper with similar evolution for the group-III element boron. The many observed allotropes of solid boron may be viewed as different packing arrangements of 12-atom icosahedral clusters.[9,10] We consider here only the simplest of these observed allotropes at atmospheric pressure, namely the α-rhombohedral phase in which there is one 12-atom icosahedron per primitive rhombohedral cell. Although not the thermodynamically stable phase,[11] α_{12}-boron (α_{12}-B) is metastable at ambient conditions, and is certainly representative of the class of icosahedral-based structures. It is an insulator with a measured gap of 2 eV.[12] Electronic-structure calculations by Bullett[13] and Switendick[14] yield indirect gaps of 1.7 and 0.23 eV, respectively, with direct gaps more than 1 eV larger. These calculations indicate the presence of covalent bonds in α_{12}-B and related structures, although the simplest two-electron-bond picture is no longer applicable.[13]

The purpose of this paper is to report first-principles total-energy calculations which predict that insulating α_{12}-B will transform first to a metallic body-centered-tetragonal phase at 210 GPa (2.1 Mbar) and then subsequently to a face-centered cubic structure at 360 GPa (3.6 Mbar). It is significant that neighboring group-III element Al is observed in the fcc structure at atmospheric pressure, as there is a general tendency for heavier members of a given group to represent high-pressure forms of lighter members.[5] This behavior follows from an increase in the size of the ion core radius relative to the atomic or Wigner-Seitz radius as one moves to heavier group members, thus effectively compressing the valence electrons between the two radii. While such a correlation is certainly valid to a first approximation, differences such as the absence of p electrons in the cores of second-period elements refine this perspective. The so-called BC-8 structure, for example, is predicted to be high pressure stable in C but not in Si.[15] Nevertheless, on the overall scale of the coordination-number dependence of the structural energies, the correspondence among C, Si, and Ge does exist; and we expect a similar correspondence among the group-III elements. Specifically, we suggest that 210 GPa is an upper bound for the onset of a sequence of structural transitions by which B evolves from a covalent insulator to a trivalent metal more like Al.

The paper is organized as follows. The total-energy calculations are described and results are presented in Sec. II. A discussion of the predicted phase transitions is given in Sec. III along with considerations of stability. We conclude with a summary in Sec. IV.

II. COMPUTATIONAL METHODS

The present total-energy calculations have been carried out using both *ab initio* plane-wave pseudopotential and linear muffin-tin-orbitals (LMTO) methods for the α_{12}-B, diamond, simple cubic (sc), face-centered-cubic (fcc), hexagonal-close-packed (hcp), and body-centered-cubic (bcc) structures, as described in the following two subsections. Only the lattice constant was varied for the α_{12}-B structure, with the rhombohedral angle and positional parameters kept fixed.[16] Similarly, only the ideal axial ratio, $c/a = \sqrt{8/3}$, was considered for the hcp structure.

Investigation of the structural stability of the fcc phase led us also to consider the body-centered-tetragonal (bct) structure[17] for a range of c/a values as well as monoclinic distortions of the fcc structure.[18] The monoclinic and bct calculations were performed only with the *ab initio* pseudopotential method.

A. Pseudopotential calculations

The pseudopotential calculations are performed within the framework of local-density-functional theory[19] applied in the momentum-space formalism.[20,21] We use nonlocal, norm-conserving,[22] *ab initio* ionic pseudopotentials as tabulated by Bachelet *et al.*[23] The Ceperley-Alder[24] model is used for the exchange-correlation potential. In addition to the total energy E, the stress tensor, the pressure p, the enthalpy $H = E + pV$, and the forces are calculated analytically from the stress theorem.[25] Details of the computational procedure have been documented in the literature.[21]

Boron is an element for which a pseudopotential description should be adequate because the core $1s^2$ states do not overlap significantly with the valence states. However, since the core of boron consists only of $1s^2$ states, there is no cancellation for the p and d states in the core region and, consequently, the resulting pseudopotentials are deep for these angular-momentum channels. As a result, a correct description of the boron pseudofunction requires a large number of plane waves.

Pseudopotential calculations were performed on a large number of structures: sc, bcc, fcc, diamond, ideal hcp, bct with various values of c/a, monoclinic distortions[18] of fcc for various angles, and α_{12}-B in which, as noted above, only the lattice constant was varied.[16] In the results presented below, the wave function is expanded in a set of plane waves. A kinetic energy cutoff of 70 Ry was used for all the simple metallic phases: sc, bcc, fcc, diamond, bct, monoclinic, and hcp structures. A kinetic energy cutoff of 50 Ry was used for the description of the α_{12}-B structure.[26] Special **k** points were generated using the Monkhorst-Pack algorithm.[27,28]

Simultaneous evaluation of the total energy E and of the pressure p as a function of atomic volume V allows a systematic monitoring of the level of convergence realized. For a fully converged calculation, the equilibrium atomic volume V_0 extracted from the minimum of the calculated $E(V)$ relation and from the $p(V_0) = 0$ zero-pressure condition should be identical.[29] We have assured adequate convergence of our calculated ground-state properties by explicitly verifying that the calculated $p(V)$ and $E(V)$ curves yielded essentially the same value of the equilibrium atomic volume V_0 and values of the bulk modulus B_0 to within 5%. This condition provides a test for the internal consistency and accuracy of the calculations.

The results of our *ab initio* plane-wave pseudopotential calculations are indicated in Fig. 1 where the calculated total energy is plotted as a function of the atomic volume

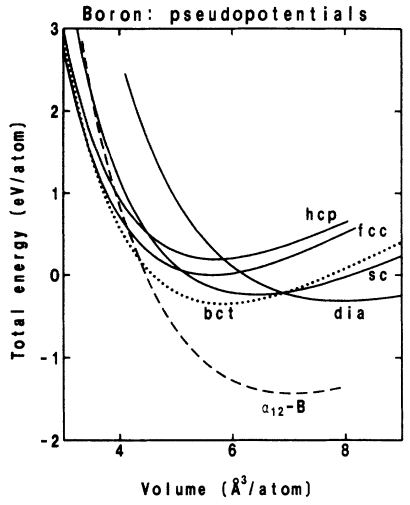

FIG. 1. Results of *ab initio* plane-wave pseudopotential calculations of the total energy of boron as a function of atomic volume for the α_{12}-B, body-centered-tetragonal (bct) with an axial ratio $c/a = 0.65$, diamond (dia), simple cubic (sc), face-centered-cubic (fcc), and ideal hexagonal-close-packed (hcp) structures. All calculations were performed with a kinetic energy of 70 Ry except in the case of α_{12}-B, where a cutoff of 50 Ry was used for atomic volumes $V < 5$ Å^3 and an extrapolation from 35 to 50 Ry was used for illustration purposes at atomic volumes $5 < V < 8$ Å^3. The zero of energy coincides with the minimum energy of the fcc structure.

for the metallic sc, fcc, bct, diamond, hcp, and insulating α_{12}-B structures. The bct structure is characterized by $c/a = 0.65$. The choice of this value is based on stability considerations for the fcc structure and is discussed in Sec. III. Similarly, results for the monoclinic distortions are discussed in Sec. III and are not shown in Fig. 1 since our calculations indicate that these are never high pressure stable. The total energy for the bcc structure is higher than the fcc structure at all atomic volumes and is not shown in Fig. 1 for purposes of clarity.

The corresponding values of the equilibrium atomic volume V_0, bulk modulus B_0, and cohesive energy E_0 are listed in Table I for all the structures studied. The values indicated in Table I are obtained by fitting the calculated total energies to Murnaghan's equation of state[30]

$$E_{\text{total}}(V) = E_0 + \left(\frac{B_0 V}{B_0'}\right)\left(\frac{(V_0/V)^{B_0'}}{B_0' - 1} + 1\right) . \quad (1)$$

For each crystal structure, the fits to Murnaghan's equation of state were performed using at least six values of the total energy calculated for lattice constants near the equilibrium volume. For all the fits, the rms errors were typically smaller than 10^{-4} eV/atom.

Inspection of Fig. 1 reveals the occurrence of two phase transformations α_{12}-B $\rightarrow$ bct $\rightarrow$ fcc leading to a covalent-metallic transition. Calculation of the enthalpy[31] for the fcc, bct, and α_{12}-B phases indicates that the transition

TABLE I. Equilibrium atomic volume V_0, bulk modulus B_0, and energy E_0 extracted from a fit of the $E(V)$ curves shown in Figs. 1 and 2 for seven crystal structures of boron. The first number for each category was calculated using the *ab initio* plane-wave pseudopotential method; the second, the LMTO method. Experimental results for B are in parentheses: The value for V_0 (Ref. 16) is for α_{12}-B, while that for B_0 (Ref. 42) is for an unspecified phase.

structure	atomic volume V_0 (Å^3)	bulk modulus B_0 (Mbar)	energy E_0 (eV/atom)
bcc	5.88	2.37	0.38
	6.12	2.32	0.29
hcp	5.72	2.68	0.19
$c/a = \sqrt{8/3}$	5.99	2.55	0.18
fcc	5.65	2.69	0.00
	5.91	2.66	0.00
sc	6.43	2.41	-0.24
	6.65	2.43	-0.35
diamond	7.93	1.86	-0.32
	8.23	1.86	-0.42
bct	5.85	2.82	-0.35
$c/a = 0.65$	6.27	2.63	-0.24
α_{12}-B	7.05	2.49	-1.43
	6.93	2.66	-1.83
experiment	(7.28)	(2.0)	

pressures are $p_{\text{trans}} = 210$ GPa for the α_{12}-B $\rightarrow$ bct transition and $p_{\text{trans}} = 360$ GPa for the bct $\rightarrow$ fcc transition. The initial (final) volumes are 4.65 (4.02) Å^3 for the α_{12}-B $\rightarrow$ bct transition, and 3.48 (3.37) Å^3 for the bct $\rightarrow$ fcc transition. In the absence of the bct structure, these results would predict an α_{12}-B $\rightarrow$ fcc transition at 230 GPa with an initial (final) volume of 4.52 (3.77) Å^3.

Due to computer core memory limitations it is not possible to carry out calculations for the α_{12}-B structure to atomic volumes greater than ≈ 5 Å^3 at a kinetic energy cutoff of 50 Ry. However, the utilization of a 35 Ry cutoff is possible up to an atomic volume of 8 Å^3. Consequently, we have performed convergence tests for the α_{12}-B structure at small atomic volumes in order to extrapolate total energies at large volumes. These tests reveal that the utilization of kinetic energy cutoffs larger than 25 Ry simply leads to a rigid downward shift of the $E(V)$ curve without appreciably modifying the equilibrium atomic volume or the bulk modulus. For the purpose of illustrating the complete $E(V)$ curve for α_{12}-B, we have extrapolated our calculations from 35 to 50 Ry for atomic volumes $5 < V < 8$ Å^3 to obtain the α_{12}-B curve shown in Fig. 1. We emphasize that this extrapolation has no effect on the numerical determination of the transition pressures since these pressures are extracted form enthalpy calculations at small atomic volumes for which a 50-Ry cutoff was used.

B. LMTO calculations

The present LMTO (Refs. 32 and 33) calculations for the high-symmetry diamond, sc, fcc, hcp, and bcc structures were carried out as described in detail elsewhere.[34] The calculations were non-relativistic, employed the von Barth–Hedin exchange-correlation potential,[35] retained *s-d* basis functions, and included Andersen's combined correction.[32,33] Empty spheres were used for the diamond and sc structures, and the Ewald or muffin-tin correction was added to the total energy in all cases.[34] All five electrons were treated in band mode, with one panel for the 1*s* and another panel for the combined 2*s*, 2*p* states. The upper panel was sampled with 89 (diamond), 165 (sc), 240 (fcc), 80 (hcp), and 140 (bcc) points per irreducible wedge of the respective Brillouin zones.

The α_{12}-B and bct structures require more complicated dispositions of atomic and empty spheres, but were otherwise treated in a similar manner. Sixteen spheres of five inequivalent types were used for the primitive rhombohedral cell of α_{12}-B: six B(1) and six B(2) atom-based spheres,[16] one $E(1)$ empty sphere at $(0,0,0)$, two $E(2)$ spheres at $\pm(0.25,0.25,0.25)$, and one $E(3)$ sphere at $(0.5,0.5,0.5)$. The relative radii were 1, 1.040, 0.944, 1.053, and 1.457, respectively. Five spheres of two inequivalent types were used for the primitive bct cell: one atom-based sphere at $(0,0,0)$, and four empty spheres at $(\pm x,0.5,0)$ and $(0.5,\pm x,0)$ where $x = 0.25/(1+c/a)$. The relative radii were $c/2a$ and x, respectively. The Brillouin zones were sampled with 13 (α_{12}-B) and 169 (bct) points per irreducible wedge, with the small α_{12}-B sampling permitted by its insulating nature. Standard expressions for the Ewald correction[34] were generalized to the case of unequal sphere radii for the α_{12}-B and bct structures, and in both cases the minimum electron density ρ_c used in this correction was found at the center of empty spheres.

Our LMTO total-energy curves for the six structures are presented in Fig. 2; the equilibrium properties are presented on the second line for each structure in Table

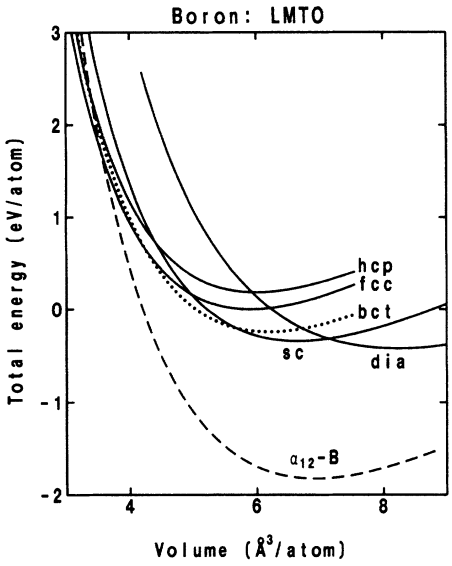

FIG. 2. Results of LMTO calculations of the total energy of boron as a function of atomic volume for the α_{12}-B, body-centered-tetragonal (bct) with an axial ration $c/a = 0.65$, diamond (dia), simple cubic (sc), face-centered-cubic (fcc), and ideal hexagonal-close-packed (hcp) structures. The zero of energy coincides with the minimum energy of the fcc structure.

I. The effect of the combined correction has been to increase the LMTO equilibrium volumes V_0 (energies E_0) in Table I by 22% (2.3 eV), 8.3% (0.42 eV), and 6.8% (0.45 eV) for the more important α_{12}-B, bct, and fcc structures, respectively. The Ewald correction has contributed additional increases of $\approx 3\%$ (≈ 0.3 eV) for the bct, fcc, hcp, and bcc phases, while leaving the more open-packed α_{12}-B, diamond, and sc results largely unchanged.

Comparison between Figs. 1 and 2, and inspection of Table I, reveal good agreement between *ab initio* pseudopotential and LMTO results for the five high-symmetry structures, as has previously been documented for the case of C and Si.[34] We expected and found evidence of inaccuracies in the LMTO total energies for the low-symmetry α_{12}-B and bct structures, due to the shape approximation used in the present implementation of this method.[36]

One indication of the shape-approximation inaccuracies is disagreement between $-dE/dV$ and the virial-theorem-derived pressure for low-symmetry structures when the combined correction is used. This correction uses a pseudo-wave-function to correct the one-electron matrix elements from the atomic spheres to the proper nonoverlapping polyhedra. The pseudo-wave-function is fit to the self-consistent wave function only at the sphere boundaries, yet it must be used far away from this region in low-symmetry cases, which interferes with the self-consistency required for satisfaction of the virial theorem. Thus while the minimum-energy and virial-theorem $3pV = 0$ derived values of V_0 agree to better than 2% for the five high-symmetry structures, the former value of V_0 is 3.9% and 8% larger than the latter for the bct ($c/a = 0.65$) and α_{12}-B structures, respectively. We have found the calculated total energy to be more accurate than the virial-theorem-derived pressures for the lower-symmetry structures,[37] and therefore have used the $E(V)$ curves exclusively for the LMTO results in this paper.

It is to be emphasized that the present LMTO calculations do clearly predict an α_{12}-B $\rightarrow$ fcc transition in B in the same volume range as the *ab initio* pseudopotential method. The absence of an intervening bct phase in Fig. 2 is no surprise given the inaccuracies to be expected for the low-symmetry bct, and especially the α_{12}-B structures given the shape approximation made in these LMTO calculations.[36,38] For this reason we defer to the pseudopotential results indicated in Fig. 1 for a quantitative determination of the transition pressures.

The electronic band structure of α_{12}-B appears to be far less sensitive to the shape approximation than is the total energy, as has been noted by Switendick.[14] The present LMTO calculations yield an ≈ 1 eV, indirect, insulating gap in α_{12}-B at large volumes, which closes at $V = 3.6$ Å^3. Prior to closure, the state just above (below) the gap lies 77% (100%) within the B spheres, which contain 67% of the cell volume. Thus in close analogy to diamond-phase Si,[5] gap closure in α_{12}-B also arises from *itinerant*, antibonding, conduction states becoming energetically more favorable than *localized*, bonding, valence-band states. Loss of the hybridization gap in α_{12}-B signals a deterioration of the covalent bond in this phase, which is clearly related to its loss of stability at high pressure.

III. PHASE TRANSITIONS AND FCC STABILITY

The *ab initio* pseudopotential and LMTO total-energy curves presented in Figs. 1 and 2 are in good overall qualitative agreement, and both predict that a fcc phase of B will become more stable than α_{12}-B at high pressures. As previously noted, we believe the primary quantitative differences between the two methods as implemented here arise from shape-approximation inaccuracies in the LMTO-calculated α_{12}-B and bct results. For this reason we draw our quantitative predictions from the *ab initio* pseudopotential calculations in Fig. 1, which indicate an α_{12}-B $\rightarrow$ bct transition at 210 GPa followed by a bct $\rightarrow$ fcc transition at 360 GPa.

We now describe the structural stability of the fcc phase and how such an analysis led us to consider tetragonal and monoclinic distortions of this phase. Stability of the fcc structure was first investigated by means of pseudopotential calculations of the elastic constants c_{11}, c_{12}, and c_{44}. The most striking result was a negative value of c_{44} at the equilibrium atomic volume ($V_{\text{fcc}} = 5.65$ Å^3), indicating that the fcc structure is unstable against shear of the unit cell at that atomic volume. Such a shear is realized by a monoclinic distortion of the unit cell.

Total-energy calculations for monoclinic distortions[18] of the fcc unit cell were then carried out as a function of the angle γ between the a and b axes of the unit cell, where $\gamma = 90°$ corresponds to the fcc structure. Results of these pseudopotential calculations are shown in Fig. 3(a) for atomic volumes $V = 5.65$ Å^3 (dashed curve) and 3.91 Å^3 (solid curve). The former is the fcc equilibrium volume V_{fcc}; the latter is the fcc volume at 200 GPa. Our results indicate that the fcc structure is unstable against a monoclinic distortion at the equilibrium atomic volume but becomes stable against such distortions for $V < 3.9$ Å^3. A similar situation has been documented for rhombohedral distortions of the sc structure in the case of P (Ref. 7) and As.[8]

The $\gamma \approx 65°$ minimum of the dashed curve in Fig. 3(a) is a body-centered orthorhombic structure[18] whose first and second neighbors closely approximate in number and distance those of a bct structure with $c/a = 0.58$. Since other group-III members Al ($c/a = \sqrt{2}$, i.e., fcc), high-pressure β or Ga-II ($c/a = 1.59$), and In ($c/a = 1.52$) assume structures within the bct family,[9] we have also investigated tetragonal distortions[17] of fcc over a wide range of c/a values.

Our pseudopotential calculations for the total energy of the bct structure as a function of c/a are shown in Fig. 3(b). Results are presented for the same two volumes as in Fig. 3(a), and in addition for $V = 3.0$ Å^3 (dotted curve), which is well into the region of fcc stability. The dashed curve at $V_{fcc} = 5.65$ Å^3 is consistent with local minima at $c/a = \sqrt{2}$ and another at slighly smaller c/a. More important, however, is the global minimum at $c/a \approx 0.6$, which is the lowest energy we have found at V_{fcc} for structures other than α_{12}-B. As the atomic volume is reduced, this minimum shifts to slighly larger c/a values and becomes less deep, until at $V \approx 3.5$ Å^3 it rises above the fcc minimum which then becomes the global bct minimum as a function of c/a. In the range of the α_{12}-B $\rightarrow$ bct $\rightarrow$ fcc transitions, the bct minimum occurs for $c/a \approx 0.65$, which is the reason we have used this value of c/a in Figs. 1 and 2.

It is interesting to note that most of the qualitative features evident in Fig. 3(b) have been observed in bct calculations for other polyvalent metals, for example, divalent Hg,[39] trivalent In,[40] and tetravalent Sn.[41] Generally there is a local maximum at the bcc structure ($c/a = 1$) and a local minimum in the range $c/a = 0.6 - 0.9$. The latter corresponds to the observed high-pressure β and γ phases of Hg (Ref. 39) and Sn,[41] respectively, and our predicted high-pressure bct phase of B. On the high c/a side of the bcc maximum, there is usually a fcc ($c/a = \sqrt{2}$) local minimum and possibly others close by ($c/a = \sqrt{2} \pm 0.2$), as in δ-Hg (Ref. 39) and the observed Ga-II and In structures.[40] Our B results in Fig. 3(b) suggest such an additional minimum for V_{fcc}, however not at the two smaller volumes.

Turning to the accuracy of our predictions, it is to be noted that similar local-density-functional calculations have been quite successful in accounting for high-pressure structural phase transitions in other solids.[5–8] While the

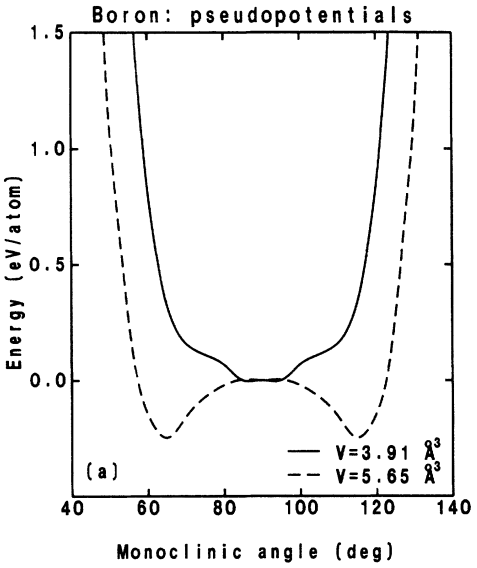

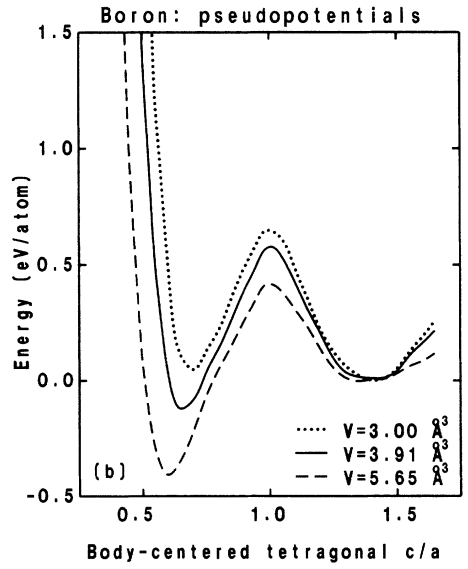

FIG. 3. Results of *ab initio* pseudopotential calculations for the monoclinic and body-centered-tetragonal phases of boron. All calculations were performed with a kinetic energy of 70 Ry. (a) Calculated total energy of boron as a function of the monoclinic angle γ for a special case of the monoclinic structure in which $a = b = c$ for different atomic volumes. (b) Calculated total energy of boron as a function of the c/a ratio for the body-centered-tetragonal structure for different atomic volumes. Atomic volumes are 5.65 Å^3 (dashed curves), 3.91 Å^3 (solid curves), and 3.00 Å^3 (dotted curve). The first is the fcc equilibrium volume, the second corresponds to a fcc pressure of 200 GPa, and the third is well into the fcc stability regime. The minimum energy of the fcc structure (at the particular atomic volume shown) is chosen as the zero of energy.

α_{12}-B structure is numerically more challenging, agreement with the measured bulk properties in Table I is consistent with expectations based on this experience. The *ab initio* pseudopotential equilibrium volume for α_{12}-B is within 3% of experiment,[16] for example. The corresponding bulk modulus is 27% larger than experiment;[42] however, the data are for an unspecified phase of B which is quite likely not α_{12}-B.

Based on an all-electron, spin-polarized atom calculation, we obtain a LMTO value for the α_{12}-B cohesive energy of 7.4 eV/atom. Using the E_0 values in Table I, we can estimate an *ab initio* pseudopotential value for the α_{12}-B cohesive energy of 7.0 eV/atom, which compares to the measured 5.9 eV/atom value again for an unspecified phase.[43] An overbinding of ≈ 1 eV/atom is not unusual in local-density calculations for second-period elemental solids, as for example diamond phase C.[34] These errors most likely arise from an inadequate treatment of the atom,[44] which will not affect calculations of phase transtions within the solid.

Another source of uncertainty in our predictions is the possibility of intervening phases not considered here. It has not been the purpose of this exploratory work to carry out an exhaustive study of potential high-pressure phases of B. Rather, we assert that the 210-GPa pressure of our predicted α_{12}-B $\rightarrow$ bct transition sets the scale for the pressure-induced loss of covalency in this material in a regime accessible by modern diamond-anvil-cell technology.

IV. SUMMARY

Results of first-principles total-energy calculations suggest that covalent, insulating α_{12} boron will transform first to a metallic body-centered-tetragonal structure at approximately 210 GPa and subsequently to a face-centered-cubic structure at approximately 360 GPa. These transitions accompany the deterioration of the covalent bond within the α_{12} phase as indicated by loss of its hybridization gap with increasing pressure. While the possibility of intervening phases not considered here cannot be ruled out, we argue that 210 GPa is an upper bound for the onset of a sequence of structural transitions by which boron evolves from a covalent insulator to a trivalent metal more like its neighbor Al. Such transitions are experimentally accessible to modern diamond-anvil-cell technology.

ACKNOWLEDGMENTS

The authors are indebted to K. Kunc, O. H. Nielsen, R. J. Needs, and R. M. Martin, whose pseudopotential plane-wave developments we have used. We thank J. Pastine for suggesting the present problem, and J. A. Moriarty for helpful conversations. This work has been supported by the Lawrence Livermore National Laboratory under Contract No. W-7405-ENG-48 to the U. S. Department of Energy.

[1] H. Olijnyk, S. K. Sikka, and W. B. Holzapfel, Phys. Lett. **103A**, 137 (1984); J. Z. Hu and I. L. Spain, Solid State Commun. **51**, 263 (1984).

[2] Y. K. Vohra, K. E. Brister, S. Desgreniers, A. L. Ruoff, K. J. Chang, and M. L. Cohen, Phys. Rev. Lett. **56**, 1944 (1986).

[3] J. C. Jamieson, Science **139**, 129 (1963); T. Kikegawa and H. Iwasaki, Acta Crystallogr. B **39**, 158 (1983);

[4] T. Kikegawa and H. Iwasaki, J. Phys. Soc. Jpn. **56**, 3417 (1987).

[5] A. K. McMahan, Physica B+C **139&140B**, 31 (1986).

[6] M. T. Yin and M. L. Cohen, Phys. Rev. B **26**, 5668 (1982).

[7] D. Schiferl, Phys. Rev. B **19**, 806 (1979); K. J. Chang and M. L. Cohen, *ibid.* **33**, 6177 (1986).

[8] R. J. Needs, R. M. Martin, and O. H. Nielsen, Phys. Rev. B **33**, 3778 (1986); L. F. Mattheiss and D. R. Hamann, *ibid.* **34**, 2190 (1986); K. Shindo, T. Sasaki, and N. Orita, J. Phys. Soc. Jpn. **58**, 924 (1989).

[9] J. Donohue, *The Structures of the Elements* (Wiley, New York, 1974), p. 48.

[10] *Boron-Rich Solids*, AIP Conf. Proc. No. 140, edited by D. Emin, T. Aselage, C. L. Beckel, I. A. Howard, and C. Wood (American Institute of Physics, New York, 1986).

[11] See, e.g., H. L. Yakel, in Ref. 10, p. 97.

[12] F. H. Horn, J. Appl. Phys. **30**, 1611 (1959).

[13] D. W. Bullett, in Ref. 10, p. 249; J. Phys. C **15**, 415 (1982).

[14] A. C. Switendick, in *Novel Refractory Semiconductors*, Vol. 97 of *Materials Research Society Symposium Proceedings*, edited by D. Emin, T. L. Aselage, and C. Wood (MRS, Pittsburgh, 1987), p. 45.

[15] M. T. Yin, Phys. Rev. B **30**, 1773 (1984); R. Biswas, R. M. Martin, R. J. Needs, and O. H. Nielsen, *ibid.* **30**, 3210 (1984).

[16] We use the structural data for α_{12}-B given in Table 5-5 of Ref. 9, due to Decker and Kasper. The rhombohedral angle $\alpha = 58.06°$, while the B atoms are located at $\pm(xxz)$, $\pm(xzx)$, and $\pm(zxx)$. For the six B(1) atoms, $x = 0.0104$, $z = -0.3427$; while for the six B(2) atoms, $x = 0.2206$, $z = -0.3677$.

[17] Note that a face-centered-tetragonal (fct) structure is identical to a body-centered-tetragonal (bct) structure with $a_{\rm bct} = a_{\rm fct}/\sqrt{2}$ and $c_{\rm bct} = c_{\rm fct}$.

[18] Monoclinic distortions of the fcc structure were considered for the special case where $a = b = c$ and therefore correspond to body-centered orthorhombic structures.

[19] See, for example, *Theory of the Inhomogeneous Electron Gas*, edited by S. Lundqvist and N. M. March (Plenum, New York, 1983).

[20] J. Ihm, A. Zunger, and M. L. Cohen, J. Phys. C **12**, 4409 (1979).

[21] O. H. Nielsen and R. M. Martin, Phys. Rev. B **32**, 3792 (1985).

[22] D. R. Hamann, M. Schlüter, and C. Chiang, Phys. Rev. Lett. **43**, 1494 (1979).

[23] G. B. Bachelet, D. R. Hamann, and M. Schlüter, Phys. Rev. B **26**, 4199 (1982).

[24]D. M. Ceperley and B. J. Alder, Phys. Rev. Lett. **45**, 566 (1980).
[25]O. H. Nielsen and R. M. Martin, Phys. Rev. Lett. **50**, 697 (1983); Phys. Rev. B **32**, 3780 (1985).
[26]At the equilibrium atomic volume, these kinetic energy cutoffs correspond approximately to the following number of plane waves *per atom*: 430 (sc), 390 (bcc), 390 (fcc), 540 (diamond), 380 (hcp), 380 (monoclinic), and 400 (bct).
[27]H. J. Monkhorst and J. D. Pack, Phys. Rev. B **13**, 5188 (1976).
[28]For the metallic structures the following number of special **k** points were used: 56 (sc), 68 (bcc), 60 (fcc), 60 (diamond), 80 (hcp), 94 (monoclinic), and 56 (bct). For the insulating α_{12}-B structure, 10 special **k** points were used.
[29]P. Gomes Dacosta, O. H. Nielsen, and K. Kunc, J. Phys. C. **19**, 3163 (1986).
[30]F. D. Murnaghan, Proc. Natl. Acad. Sci. **30**, 244 (1944).
[31]The pressure p entering the expression of the enthalpy $H = E+pV$ was calculated independently (1) from the quantum-mechanical stress and (2) from the volume derivative of the Murnaghan fit to the energy. Both procedures yield essentially the same transition pressure.
[32]O. K. Andersen, Phys. Rev. B **12**, 3060 (1975).
[33]H. L. Skriver, *The LMTO Method* (Springer, Berlin, 1984).
[34]A. K. McMahan, Phys. Rev. B **30**, 5835 (1984).
[35]U. von Barth and L. Hedin, J. Phys. C **5**, 1629 (1972).
[36]Formulations of the LMTO method without shape approximations have recently been developed, e.g., M. Methfessel, C. O. Rodriguez, and O. K. Andersen, Phys. Rev. B **40**, 2009 (1989); however, we have not yet implemented these capabilities.
[37]The effect of the combined correction on the virial theorem may be easily demonstrated by carrying out bct calculations without empty spheres as c/a is decreased below unity. In another test, we have examined minimum-energy and virial-theorem $3pV = 0$ derived values of V_0 as a function of S_E/S_A, where S_E and S_A are radii of empty and atom-based spheres for the sc structure. We find the energy-derived values to be less sensitive to S_E/S_A and in better agreement with the optimal $S_E/S_A = 1$ result.
[38]The present LMTO calculations do predict a $c/a \approx 0.7$ minimum in the high-pressure bct energy as a function of c/a, in good agreement with the $c/a = 0.65$ *ab initio* pseudopotential minimum.
[39]J. A. Moriarty, Phys. Lett. **131A**, 41 (1988).
[40]V. Heine and D. Weaire, Solid State Phys. **24**, 250 (1970). See Fig. 74.
[41]J. Hafner, Phys. Rev. B **10**, 4151 (1974).
[42]*LASL Shock Hugoniot Data*, edited by S. P. Marsh (University of California, Berkeley, 1980), p. 24.
[43]R. Hultgren, P. D. Desai, D. T. Hawkins, M. Gleiser, K. K. Kelley, and D. D. Wagman, *Selected Values of the Thermodynamic Properties of the Elements* (Am. Soc. Metals, Metals Park, Ohio, 1973), p. 55.
[44]J. A. Moriarty, Phys. Rev. B **19**, 609 (1979). When corrected for spin polarization, the results shown in Table I of this reference suggest that local-spin-density calculations will underestimate the valence binding energy of the second-period atoms B and C by 0.7 and 1.0 eV, respectively, while making errors an order of magnitude smaller for the third-period atoms Al and Si. These errors are in the direction to improve local-density-calculated cohesive energies for second-period solids.